Iron Minerals in Bath Stone (Great Oolite, Middle Jurassic, UK): Pyrite, Goethite and Glauconite, their Spectra and Origins

By

Maurice Tucker & Robert Fosbury
maurice.tucker@bristol.ac.uk
Earth Sciences, University of Bristol, BS8 1RJ.
bobfosbury@gmail.com
Astronomer Emeritus, European Southern Observatory; Hon. Prof., UCL Inst. Ophthalmology.

Bath Stone, so familiar to all who live in or visit Bath, is an oolitic limestone (in the Great Oolite Group) deposited in a shallow sea like that in the Bahamas now, around 167 million years ago in Middle Jurassic time. Bath Stone has been extracted from open and underground quarries around the city for nearly 2000 years, since the Romans arrived here and started building Aquae Sulis and their baths about 45 CE. Although Bath Stone is a very pure limestone, composed of just calcite and a little clay, there are iron minerals present in the rock. We describe the presence of pyrite (now replaced by goethite) but also report the surprising and rare occurrences of glauconite, a mineral common in the Cretaceous greensands, identified by visible-IR reflectance. We discuss the formation of these minerals within the oolitic sediment and note the potential value of a high-fidelity spectral bio-marker from the Middle Jurassic.

Pyrite

Pyrite is a common mineral in sedimentary rocks, especially in organic-rich mudrocks, and it is commonly dispersed in limestones. Within the Bath Stone, there are dark, mm-size, metallic looking crystals scattered in the rock but they do also occur in discrete areas (Fig. 1a). These crystals are referred to as 'shot' by the stonemasons. In some cases, there are larger rusty-brown nodules, several cm in diameter (Fig. 1b). Although these crystals and nodules are likely to have been composed of pyrite (iron sulphide, FeS2), they are now composed of goethite (FeO(OH), see below). On close inspection the individual crystals can be seen to have a cubic shape or in some cases more of a spheroidal, framboidal shape. Fossils are not very common in the Bath Stone, apart from ubiquitous sand-sized fragments (bioclasts), but rarely pyrite is observed closely associated with bivalve or coral fossils, as in Fig. 2, where the crystals are concentrated immediately below a large shell. The more elongate patches-nodules of goethite/pyrite may relate to burrows, which were created in the sediment by crustaceans particularly.

In many places in the Bath Stone there are patches of a dull orange to reddish-brown discolouration in the vicinity of pyrite-goethite (Fig. 3). These stains in the mostly cream-coloured stone are the result of oxidation of the pyrite crystals when exposed to the atmosphere. Effectively, the pyrite, composed of the reduced form of iron (Fe2+), is 'rusting' to limonite, the hydrated form of ferric oxide-hydroxide: i.e., FeO.nH2O.

Fig. 1a: Scattered pyrite crystals. Field of view 8 cm.

Fig. 1b: An elongate nodule of pyrite crystals, likely formed within a burrow. Field of view 6 cm. Bath Stone, Bath Riverside.

Fig. 2: A bivalve shell with pyrite crystals developed just beneath the shell. At 10-15 mm below the pyrite there are scattered green grains at a similar level, interpreted as glauconite. Field of view 10 cm across.

Fig. 3: Orange-brown stain emanating from rusting pyrite crystals and spreading out into the oolitic limestone. Field of view 15 cm across.

Glauconite

Glauconite is another iron mineral found in sedimentary rocks, but it is a silicate, related to the clay minerals (phyllosilicates); it also contains potassium and magnesium. It has a complicated formula KMg(FeAl)(SiO3)6. 3H2O and the iron here is present in both the ferric (Fe3+, also written as Fe (III)) and ferrous (Fe2+, Fe (II)) valence states. Glauconite is especially common in the greensands of the Cretaceous, well exposed in road cuttings at Potterne, just south of Devizes for example, at Cley Hill near Warminster and in the Vale of Wardour near Dinton. Greensand has been used locally as a building stone, as in Mere and villages around Shaftesbury. It is known as Hurdcott Stone and is still quarried near Tisbury (see Geddes 2011).

Glauconite has a distinctive green colour in thin-section (Fig. 4); it is usually pleochroic, with an aggregate polarisation pattern. In many cases the sand-sized grains are ovoid-shaped and these are often interpreted as glauconite-impregnated faecal pellets. In some cases, glauconite occurs within microfossils, such as foraminifera.

Fig. 4: Photomicrograph of glauconite grains along with quartz grains in Greensand, Dorset. Plane polarised light. Field of view 8 mm across.

Millimetre-size grains of glauconite have been found (with the aid of a hand-lens) in the Bath Stone of several buildings and walls around the city: at Bath Riverside, in York Street and in Denmark Road East Twerton for instance. These grains are mostly spheroidal to ellipsoidal in shape, 0.5 to 1 mm in diameter (Fig. 5), but a thin flaky clay-like variety is also present (Fig. 6). The grains appear to be scattered within the oolitic sediment, rather than concentrated in laminae or lenses. In one particular occurrence at Bath Riverside, these green grains are located in the oolitic sand along a level of about 10-15 mm below the convex-upward bivalve shell which is forming an 'umbrella structure' in the limestone where pyrite is present immediately below the shell itself (Fig. 2). Green grains have also been observed in the Fuller's Earth Rock, the limestone 10 m below the Bath Stone, from Winsley. In addition, Sellwood et al. (1985) recorded glauconite in the Great Oolite Humbly Grove reservoir in Sussex.

Fig. 5: Close-up of glauconite grains in Bath oolite. Field of view 8 mm across.

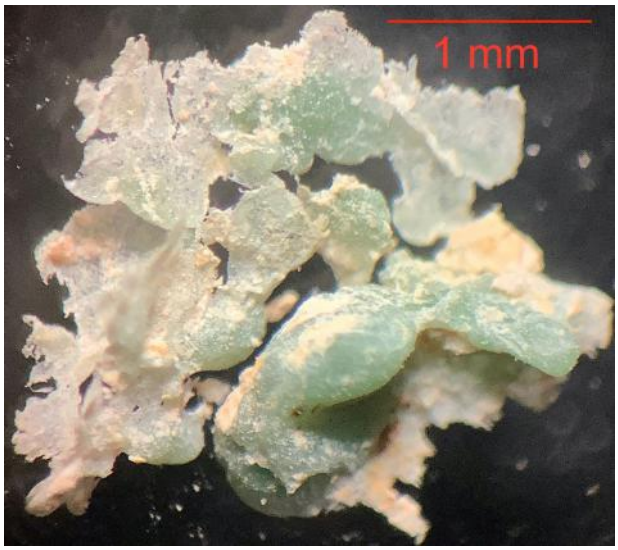

Fig. 6: Green and flaky grains extracted from Bath oolite interpreted as glauconite. Our experiments focused on the largest grain at the bottom right of this image.

Identifying the green grains as glauconite just from their colour and shape is clearly not conclusive, although there are no other obviously green, sand-size minerals that might occur in sedimentary rocks. Mafic minerals like olivine and pyroxene which might be green are very unlikely to occur in the Bath oolite, since there are no igneous rocks as a source in the region and such mafic minerals anyway are extremely rare as reworked grains. Other green minerals such as the clay chlorite are typically flakes; another green mineral is celadonite, also flaky, but that is derived from alteration of basalt.

Unfortunately, we do not have sufficient material to prepare a thin-section for petrographic studies. However, there are two non-destructive techniques that can be applied to grains with a view to determining their mineralogy: X-Ray Diffraction and Visible-IR Spectroscopy. We did try XRD, but the peaks obtained did not confirm the mineral. This could be a consequence of just using the few grains we had (rather than grinding them into a powder) or the mineral itself being poorly crystallised. Visible-near-IR Spectroscopy is a technique used on individual minerals as well as in remote sensing surveys from a distance, as from a satellite, and this has been successfully applied to surveys of Mars for example (e.g., Horgan et al. 2020). In our case the use of spectroscopy confirmed glauconite but also provided some extra intriguing detail, described here.

Visible-IR Spectroscopy and mineral identification

The non-destructive use of reflection or transmission spectroscopy of translucent samples can reveal diagnostic electronic (UV and visible) or vibrational (infrared) transitions in atoms or molecules within many materials. The spectra obtained from the dark metallic crystals (shot) we interpret as pyrite actually reveal that they are composed of goethite (brown line Fig. 7). As noted earlier, this mineral will have formed by oxidation of the pyrite.

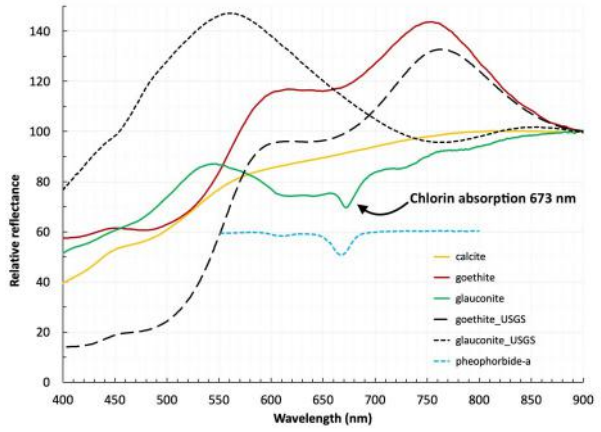

Fig. 7: Visible reflectance spectra. The unbroken coloured lines show the relative reflectance spectra, normalised at 900 nm, of the three minerals: yellow — Bath oolite (calcite); brown— goethite (after oxidised pyrite), and green — the largest grain of the green material glauconite). The prominent absorption line at 673 nm, identified as a chlorophyll derivative, is marked with an arrow. The spectra shown for comparison are samples of: goethite (long-dashed black) and glauconite (short-dashed black), both from the US Geological Survey spectral database, and in dashed blue, a transmission spectrum of the chlorophyll derivative, pheophorbide-a in ethanol, with a concentration and sample depth adjusted to provide a similar strength absorption close to 670 nm from a biological chlorin.

For a translucent sample like the Bath green grains, the reflectance signal is dominated by light that has entered the material and emerged after single or multiple scattering within it. In practice, there is little difference between the signal in reflected or transmitted light. To examine the small green grains in the Bath Stone, we used reflectance spectroscopy covering the range from 400 to 2500 nm. Given their small size, we generated a small, 0.2 mm diameter, high-intensity spot on the stage of a microscope. Light from an Ocean Insight HL-2000 halogen visible/near-IR lamp, fed with a collimated fibre, illuminated the back of a low-power microscope objective. The sample was then placed precisely within the spot using the microscope x-y stage and focus controls. Scattered light was collected from the illuminated fragment with a second collimated fibre aimed at the sample using a micro-manipulator. This setup allowed the collection of high-quality visible spectra from the grains using an Ocean Insight Maya2000Pro (200–1100 nm) spectrometer with a resolution (FWHM) of 2 nm. For the IR spectrum, an Ocean Insight NirQuest (900–2500 nm) spectrometer with IR-transmitting fibres and collimator was used. For this wavelength range the microscope optics could not be used so we were unable to achieve such a high signal-to-noise ratio. The same HL-2000 lamp was employed for both ranges. The resolution of the IR data is a factor of 4 or more lower than for the visible range. To calibrate the reflectance, an Ocean Insight WS-1 diffuse reflectance standard was used over the entire wavelength range. Given the different modes of illumination and sample structures, our reflectances are reported as relative rather than absolute values (i.e., the plots can be arbitrarily scaled vertically).

In Figure 7, the broad reflectance peak (green line) from the sample centred around 540 nm is typical of glauconite and is predominantly the result of a gap between the strong broad absorptions of Fe3+ increasing the absorbance at longer and shorter wavelengths. The narrow absorption feature at 673 nm is not generally seen in glauconite samples and this led us to an intensive search for possible identifications of this prominent signature. The only narrow absorption feature found in rock samples that appears remotely feasible comes from chromium in the form of Cr3+, present for example in chrome diopside. Although chromium-rich glauconite is known (Bitschene et al. 1992), this identification is not convincing since the wavelength is a poor match and the Cr3+ absorption line (seen in a range of chromium-coloured gemstones including emerald, kyanite and zoisite), commonly appears with an asymmetric profile arising from a Fano resonance (https://en.wikipedia.org/wiki/Fano_resonance) that influences the absorption profile to make it asymmetric.

A more promising identification of the 673 nm absorption is with a chlorin associated with the transformation of plant material/organic matter. In the Treibs's scheme for chlorophyll degradation to petroporphyrins (Milgrom 1997), the final stage before the chlorophyll-porphyrin transition exhibits an olive-green colour and a chlorin-type absorption that is very close to our wavelength of interest. The dashed blue line in Figure 7 shows a typical absorption spectrum of a chlorophyll derivative, pheophorbide-a, but there are other chlorin candidates that differ little in wavelength.

The typical near-IR spectrum of glauconite shows prominent absorption bands near 1900 and 2300 nm and these are both seen in the sample of Cretaceous Greensand from Cley Hill in Wiltshire (dashed red line). Figure 8 shows the combined visible and near-IR spectrum of the largest green grain along with the Cley Hill comparison.

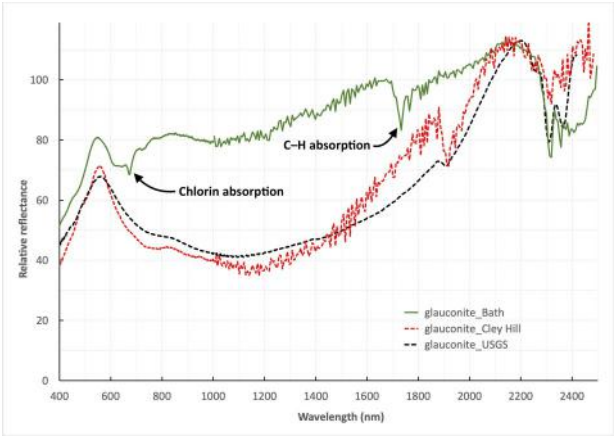

Fig. 8: Visible to near-IR reflectance spectra. The solid green line is the combination of the visible and the near-IR spectra of the largest Bath Stone green grain. The comparison spectra (dashed lines) are (black) the same USGS sample of glauconite as shown in Figure 7 and (red) the reflectance of greensand grains from Cley Hill, Wiltshire (material separated from quartz sand using a strong rare-earth magnet). The spectra of the Bath glauconite exhibit the organic absorption features at 673 nm and ~1750 nm which are both absent in typical glauconite.

In their account of the visible and near-IR remote sensing spectra of phyllosilicates, Bishop et al. (2008) ascribed the 2300 nm feature to individual OH stretching and bending modes as a function of variable octahedral cation composition. While the absorption complex around 2300 nm is present in both the Bath sample and typical glauconites, the weaker 1900 nm absorption seen in some glauconites is undetected in our Bath sample. There is instead a band between 1700 and 1800 nm that is normally identified as an overtone of the fundamental C-H vibrational stretching mode in organic materials.

By examining material that had been exposed to weathering for several years after cutting, we clearly had to ensure that our measurements were not affected by contamination from recent surface growth of organic material such as algae and/or lichens. To do this, we carefully examined the measured samples with a microscope using both visible and ultraviolet light, the latter being a sensitive test of algal chlorophyll fluorescence. Since chlorophyll itself absorbs around 670–680 nm, any presence of this must be eliminated from our measurement.

To be certain of this, we examined a second stone sample from the same mine that showed clear signs of organic surface growth. This revealed no significant red fluorescence signal but did show an absorption band at 675 nm. This band was however significantly broader and had a longer wavelength than the absorption in our green grains. In addition, the difference in absorption strength between the thick (granular) and thin (flaky) samples we measured strongly suggests that the prominent narrow absorption line at 673 nm is from the bulk green material and not from surface contamination. It should also be remarked that, while the examined material was selected by examination of the cut and subsequently exposed stone surface, most of the green material had been buried beneath the surface. We used ooid grains prised from the surface in the same way as the green grains for the calcite measurement shown in Figure 7 which shows no sign of chlorophyll contamination.

We have only found two other references to the ~670 nm chlorin absorption in sedimentary formations. These both refer to sediments in the Antarctic dry valleys. Bishop et al. (2013), in their analyses of Antarctic sediments as Mars analogue materials, recorded a sample of a dry lake sediment (H3 JB207) with an absorption feature identified as a chlorophyll-like signature. Hawes & Schwarz (2000) described the transmission characteristics of benthic microbial mats from 10 m water-depth in Lake Hoare, an ice-covered lake in the McMurdo Dry Valleys area of Southern Victoria Land, Antarctica, which show a very similar spectral structure to our BGG around 670 nm. Both of these references however refer to samples that are considerably younger than Bath Stone.

In summary, our Bath green grains show spectroscopic similarities to typical glauconite, especially the green reflectance peak near 550 nm and the IR absorption at 2300 nm. Unusually, however, they show two clear organic signatures in the form of a narrow absorption at 673 nm, most likely from a chlorophyll-derived chlorin typical of Treibs's porphyrin transformation scheme, and a C–H overtone band near 1750 nm.

Formation of pyrite and glauconite in Bath oolite

With iron precipitation, the redox of the water, i.e., the Eh, whether the water is oxidising (positive Eh) or reducing (negative Eh), is a major control on the mineralogy (Tucker 2000). In oxic water, iron is present in the insoluble ferric form, as oxide or hydroxide, commonly attached to clay minerals; the iron is only released when the water turns anoxic, and then it is ferrous iron. One of the main factors affecting the Eh of natural aqueous environments is the amount of organic matter present, since its decomposition, mainly brought about by bacteria, consumes oxygen and creates reducing conditions. Normal seawater has a positive Eh (it is oxic), as is the pore water in most surficial sediments on the seafloor. However, organic matter deposited in the sediments soon decomposes with depth so that a reducing environment is formed some 10s of cm below the sediment-water interface. Thus, an oxic seafloor and near-surface sediment pore-water passes down through a suboxic zone into an anoxic diagenetic zone. This trend is sometimes seen when digging down into beach sand near low tide, as in making a sandcastle or burying grandad, or digging for lugworms. The near-surface sand is the normal cream to pale yellow colour, but then 10-20 cm down the colour turns grey (suboxic) and then a little deeper (20-30 cm) to black (anoxic); there may also be a smell of H2S (bad eggs). This colour change is the result of microbial decomposition of organic matter in the sand and the precipitation of pyrite in the black zone where the reduced form of iron (Fe2+) is developing under the anoxic conditions, and sulphate (SO4 2-) in the pore-water is reduced to sulphide (S-).

The organic matter present within the Bath oolitic sediment will be derived from the seawater and from decomposing organisms, such as bivalves, brachiopods, etc., buried within the oolitic sediment. There may also be organic matter derived from thin biofilms growing on the seafloor, from organic matter within burrows, or from within the ooids themselves which in recent years have been interpreted as bacterial-microbial in origin, rather than being purely abiotic. The random, scattered occurrence of pyrite crystals in Bath Stone reflects the original disseminated nature of organic matter in the sediment and its decomposition to create reducing conditions which liberated iron from clays deposited with the ooids. The preferential occurrence of pyrite concentrated just beneath the shell in Figure 2, and within burrows, suggests that there was an abundance of organic matter decomposing there to generate the reducing, anoxic micro-environment wherein the pyrite precipitated.

Glauconite is a potassium-iron aluminosilicate containing both Fe (III) and Fe (II), usually with a high ferric/ferrous ratio. Glauconite is being formed on many modern continental shelves at water depths from a few 10s to 100s of m, but it is invariably a poorly-ordered phase. Glauconite forms in the sediment by the transformation of degraded clay minerals and by the authigenic growth of crystallites in the pores of substrates, be they clay minerals, skeletal grains or faecal pellets. Glauconite is commonly associated with localized occurrences of organic matter, which create local reducing conditions, but within an overall oxic environment. The occurrence of the glauconite at a level 10-15 mm below the pyrite (Fig. 4) could be a reflection of changing pore-fluid away from the anoxic conditions of the decomposing bivalve organism where the pyrite was being precipitated to more suboxic-oxic water below, allowing glauconite to form.

Oxidation of pyrite and the development of the orange-rust stains in Bath Stone

After the precipitation of the pyrite and glauconite, just below the Jurassic seafloor within the oolitic sediment, the Bath Stone was cemented and gradually buried. It would appear that the Middle Jurassic limestones in the Bath region were buried to around 500-700 metres during the Upper Jurassic, through the Cretaceous and into the Eocene. Soon after this, the area was uplifted, as a consequence of tilting towards the southeast and the effects of larger-scale plate-tectonic movements in southern Europe as a result of the closure of Tethys, the collision between Africa and Europe, and the formation of the Alpine Mountain chain. On uplift over the last 20 million years or so, the Bath oolite would have come into contact with oxic groundwaters and then the atmosphere when at the surface, such that the pyrite would become unstable and the ferrous iron sulphide would then decompose into ferric oxide-hydroxide, goethite-limonite, and give the orange-brown stains we see on the stone today.

Summary

Close observation of Bath oolite reveals the common presence of iron pyrite and the rare occurrence of glauconite. These iron minerals were precipitated within the oolitic sediment soon after deposition at a depth of several to 10s of cm below the seafloor where the appropriate micro-environments were established as a result of decomposing organic matter: anoxic conditions in the case of pyrite, and oxic-suboxic conditions in the case of glauconite. On recent uplift and contact with oxic groundwater and then subaerial exposure, the pyrite was oxidised to goethite, and weathered to give the orange-brown stains on the stone due to limonite ('rust'). Visible-IR reflectance was able to confirm the presence of goethite and glauconite although intriguingly with the latter an unexpected absorption peak was detected which could indicate the presence of degraded chlorophyll within the mineral. The presence of an additional organic spectral signature in the IR spectrum attributed to an overtone C–H vibrational absorption band is not inconsistent with this conclusion.

Acknowledgements

We are grateful to Janice Bishop (SETI Institute, California), Ian Jarvis (Kingston University, London), and others for their comments on the spectral data and to Natalie Pridmore and Hazel Sparkes (Chemistry School, Bristol) for XRD analysis.

References

Geddes, I. (2011) A Building Stone Atlas of Wiltshire. Strategic Stone Study, English Heritage.

Bishop, J.L. et al. (2008) Reflectance and emission spectroscopy study of four groups of phyllosilicates: smectites, kaolinite-serpentines, chlorites and micas. Clay Minerals 43, 35–54.

Bishop, J.L. et al. (2013) Coordinated analyses of Antarctic sediments as Mars analog materials using reflectance spectroscopy and current flight-like instruments for CheMin, SAM and MOMA. Icarus 224, 309-325.

Bitschene, P.R. et al. (1992) Composition and origin of Cr-rich glauconitic sediments from the southern Kerguelen Plateau (site 748). Proceedings of the Ocean Drilling Program, Scientific Results, Vol. 120, 113-134.

Hawes, I. & Schwartz, A-M. (2000) Absorption and utilization of irradiance by cyanobacterial mats in two ice-covered Antarctic lakes with contrasting light climates. Journal of Phycology 37, 5–15.

Horgan, B.H.N. et al. (2020) The mineral diversity of Jezero crater: Evidence for possible lacustrine carbonates on Mars. Icarus 339, 113526.

Milgrom, L.R. (1997) The Colours of Life. Oxford University Press, pp. 169-175.

Sellwood, B.W. et al. (1985) Stratigraphy and sedimentology of the Great Oolite Group in the Humbly Grove Oilfield, Hampshire. Marine & Petroleum Geology 2, 44 -55.

Tucker, M.E. (2000) Sedimentary Petrology. 3rd Edition. John Wiley, Chichester.

-.-